Article

Mononuclear Nickel(III) and Nickel(II) Thiolate Complexes with Intramolecular S–H Proton Interacting with Both Sulfur and Nickel: Relevance to the [NiFe]/[NiFeSe] Hydrogenases

Chien-Ming Lee, Chien-Hong Chen, Shyue-Chu Ke, Gene-Hsiang Lee, and Wen-Feng Liaw

J. Am. Chem. Soc., **2004**, 126 (27), 8406-8412• DOI: 10.1021/ja048568l • Publication Date (Web): 17 June 2004

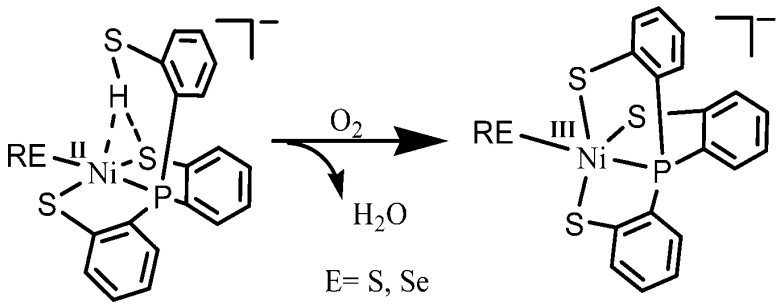

More About This Article

Additional resources and features associated with this article are available within the HTML version:

- Supporting Information
- Links to the 3 articles that cite this article, as of the time of this article download
- Access to high resolution figures
- Links to articles and content related to this article
- Copyright permission to reproduce figures and/or text from this article

View the Full Text HTML

J|A|C|S
ARTICLES
Published on Web 06/17/2004

Mononuclear Nickel(III) and Nickel(II) Thiolate Complexes with Intramolecular S−H Proton Interacting with Both Sulfur and Nickel: Relevance to the [NiFe]/[NiFeSe] Hydrogenases

Chien-Ming Lee,[†] Chien-Hong Chen,[†] Shyue-Chu Ke,*[,‡] Gene-Hsiang Lee,[§] and Wen-Feng Liaw*[,†]

Contribution from the Department of Chemistry, National Tsing Hua University, Hsinchu 30043, Taiwan; Department of Physics, National Dong Hwa University, Hualien, Taiwan; and Instrumentation Center, National Taiwan University, Taipei, Taiwan

Received March 11, 2004; E-mail: wfliaw@mx.nthu.edu.tw

Abstract: Mononuclear, distorted square planar $[Ni^{II}(ER)(P(o\text{-}C_6H_4S)_2(o\text{-}C_6H_4SH))]^-$ (ER = SePh (**1**), 2-S−C_4H_3S (**2**)) with a S−H proton directly interacting with both nickel and sulfur atoms were prepared by reaction of $[Ni(CO)(SePh)_3]^-$/$[Ni(CO)(2\text{-}S\text{-}C_4H_3S)_3]^-$ and $P(o\text{-}C_6H_4SH)_3$, individually. The presence of combinations of intramolecular [Ni−S···H−SR]/[Ni···H−SR] interactions was verified in the solid state by the observation of an IR ν_{SH} stretching band (2273 and 2283 cm^{-1} (KBr) for complexes **1** and **2**, individually) and ^1H NMR spectra (δ 8.079 (d) (CD_2Cl_2) and 8.39 (d) (C_4D_8O) ppm (−SH) for complexes **1** and **2**, respectively) and subsequently confirmed by X-ray diffraction study. The exo-thiol proton ($o\text{-}C_6H_4SH$) in complexes **1** and **2** was identified as a D_2O exchangeable proton from NMR and IR studies and was quantitatively removed by Lewis base Et_3N to yield Ni(II) dimer $[Ni^{II}(P(o\text{-}C_6H_4S)_3)]_2^{2-}$ (**5**). Instead of the ligand-based oxidation to form dinuclear Ni(II) complexes and dichalcogenide, oxidation of THF−CH_3CN solution of complexes **1** and **2** by O_2 resulted in the formation of the mononuclear, distorted trigonal bipyramidal $[Ni^{III}(ER)(P(o\text{-}C_6H_4S)_3)]^-$ (ER = SePh (**3**), 2-S−C_4H_3S (**4**)) accompanied by byproduct H_2O identified by ^1H NMR, respectively. The 4.2 K EPR spectra of complexes **3** and **4** exhibiting high rhombicities with three principal *g* values of 2.304, 2.091, and 2.0 are consonant with Ni(III) with the odd electron in the d_{z^2} orbital. Complex **3** undergoes a reversible $Ni^{III/II}$ process at $E_{1/2}$ = −0.67 V vs Ag/AgCl in MeCN.

Introduction

Hydrogenases are enzymes that catalyze the reversible heterolytic dissociation of molecular hydrogen.[1−4] [NiFe] hydrogenase containing a [Ni−Fe] center that is believed to be the catalytic site for hydrogen activation and functions more effectively in the direction of H_2 oxidation.[1−4] The X-ray crystallographic studies of the active-site structure of [NiFe] hydrogenases isolated from *D. gigas*, *D. vulgaris*, *D. fructosovorans*, and *D. desulfuricans* ATCC27774 in combination with infrared spectroscopy have revealed an active site comprised of a heterobimetallic $(S_{cys})_2Ni(\mu\text{-}S_{cys})_2(\mu\text{-}X)Fe(CO)(CN)_2$ (X = O, OH) cluster.[1−5] The bridging ligand X was proposed to be an oxide or hydroxide in the oxidized state and was found to be absent in the reduced state.[1−5] Three nonprotein diatomic groups (two cyanide and one carbonyl ligands) ligate the iron center. In the conversion between oxidized and reduced states, the iron remains low-spin Fe(II), while the Ni changes between Ni(III) and Ni(II). EXAFS/EPR studies indicate that the formal oxidation state of the Ni center is paramagnetic Ni(III) in Ni−A, Ni−B, and Ni−C states.[5−15] The catalytically active form

[†] Department of Chemistry, National Tsing Hua University.
[‡] Department of Physics, National Dong Hwa University.
[§] National Taiwan University.

(1) (a) Carepo, M.; Tierney, D. L.; Brondino, C. D.; Yang, T. C.; Pamplona, A.; Telser, J.; Moura, I.; Moura, J. J. G.; Hoffman, B. M. *J. Am. Chem. Soc.* **2002**, *124*, 281−286. (b)Albracht, S. P. J. *Biochim. Biophys. Acta* **1994**, *1188*, 167−204. (c) van der Zwaan, J. W.; Coremans, J. M. C. C.; Bouwens, E. C. M.; Albracht, S. J. P. *Biochim. Biophys. Acta* **1990**, *1041*, 101−110.
(2) (a) Volbeda, A.; Charon, M. H.; Piras, C.; Hatchikian, E. C.; Frey, M.; Fontecilla-Camps, J. C. *Nature* **1995**, *373*, 580−587. (b) Garcin, E.; Vernede, X.; Hatchikian, E. C.; Volbeda, A.; Frey, M.; Fontecilla-Camps, J.-C. *Structure* **1999**, *7*, 557−566. (c) Happe, R. P.; Roseboom, W.; Pierik, A. J.; Albracht, S. P. J. *Nature* **1997**, *385*, 126.
(3) (a) Higuchi, Y.; Yagi, T.; Yasuoka, N. *Structure* **1997**, *5*, 1671−1680. (b) Higuchi, Y.; Ogata, H.; Miki, K.; Yasuoka, N.; Yagi, T. *Structure* **1999**, *7*, 549−556.
(4) (a) Rousset, M.; Montet, Y.; Guigliarelli, B.; Forget, A.; Asso, M.; Bertrand, P.; Fontecilla-Camps, J. C.; Hatchikian, E. C. *Proc. Natl. Acad. Sci. U.S.A.* **1998**, *95*, 11625−11630. (b) Nicolet, Y.; Piras, C.; Legrand, P.; Hatchikian, C. E.; Fontecilla-Camps, J. C. *Structure* **1999**, *15*, 13−23.
(5) Matias, P. M.; Soares, C. M.; Saraiva, L. M.; Coelho, R.; Morais, J.; Le Gall, J.; Carrondo, M. A. *J. Biol. Inorg. Chem.* **2001**, *6*, 63−81.
(6) Davidson, G.; Choudhury, S. B.; Gu, Z.; Bose, K.; Roseboom, W.; Albracht, S. P. J.; Maroney, M. J. *Biochemistry* **2000**, *39*, 7468−7479.
(7) Amara, P.; Volbeda, A.; Fontecilla-Camps, J. C.; Field, M. J. *J. Am. Chem. Soc.* **1999**, *121*, 4468−4477.
(8) (a) De Lacey, A. L.; Hatchikian, E. C.; Volbeda, A.; Frey, M.; Fontecilla-Camps, J. C.; Fernandez, V. M. *J. Am. Chem. Soc.* **1997**, *119*, 7181−7189. (b) Volbeda, A.; Garcin, E.; Piras, C.; de Lacey, A.; Fernandez, V. M.; Hatchikian, E. C.; Frey, M.; Fontecilla-Camps, J. C. *J. Am. Chem. Soc.* **1996**, *118*, 12989−12996.
(9) De Gioia, L.; Fantucci, P.; Guigliarelli, B.; Bertrand, P. *Inorg. Chem.* **1999**, *38*, 2658−2662.
(10) Dole, F.; Fournel, A.; Magro, V.; Hatchikian, E. C.; Bertrand, P.; Guigliarelli, B. *Biochemistry* **1997**, *36*, 7847−7854.
(11) (a) Niu, S.; Thomson, L. M.; Hall, M. B. *J. Am. Chem. Soc.* **1999**, *121*, 4000−4007. (b) Li, S.; Hall, M. B. *Inorg. Chem.* **2001**, *40*, 18−24.
(12) (a) Stein, M.; van Lenthe, E.; Baerends, E. J.; Lubitz, W. *J. Am. Chem. Soc.* **2001**, *123*, 5839−5840. (b) Stein, M.; Lubitz, W. *Curr. Opin. Chem. Biol.* **2002**, *6*, 243−249.
(13) Maroney, M. J.; Bryngelson, P. A. *J. Biol. Inorg. Chem.* **2001**, *4*, 453−459.

10.1021/ja048568l CCC: $27.50

Ni−C of [NiFe] hydrogenase was proposed to exist as the $[(S_{cys}-H)(S_{cys})Ni^{III}(\mu\text{-}H)(\mu\text{-}S_{cys})_2Fe(CO)(CN)_2]$ with a $S_{cys}-H$ proton interacting with nickel.[8−13] Also, the architecture of the silent-active Ni−SIa is proposed as a Cys−SH proton directly interacting with nickel, $[(S_{cys}-H)(S_{cys})Ni^{II}(\mu\text{-}S_{cys})_2-Fe(CO)\text{-}(CN)_2]$.[11,12]

Interestingly, the recent X-ray crystal structures of CO-inhibited forms and single-crystal EPR studies of the reduced active site of [NiFe] H_{2ase} isolated from *D. vulgaris Miyazaki F* implicate that the Ni−C intermediate is a formal Ni(III) oxidation state with a hydride (H^-) bridging between the Ni and the Fe atoms and the sulfur atom of Cys 546 hydrogenated for the catalytic reaction of the enzyme.[14,15] Upon illumination, the Ni−C state is transformed into a fourth paramagnetic Ni−L state. These conversions are considered to correspond to photodissociation of proton species from the [Ni−Fe] center.[8−15] In addition, the active form Ni−C has also been shown to contain a solvent exchangeable proton, assigned as a Cys−SH proton directly interacting with nickel from ENDOR studies.[16] Very recently, a particularly interesting new type of hydrogenase isolated from *Ralstonia eutropha*, the so-called regulatory hydrogenase (RH), was found to belong to the subclass of H_2-sensing [NiFe] hydrogenase. The oxidation state and coordination ligands of the Ni site of RH that were investigated by X-ray absorption spectroscopy imply that a five-coordinate $[Ni^{II}-S_3(O/N)_2]$ for RH^{ox} and a six-coordinate $[Ni^{III}-S_2(O/N)_3(H)]$ for RH^{+H2}.[17,18]

In model compounds,[19] an electrochemical study provided evidence for such a Ni(III)−H species generated by one-electron reduction of a nickel(II) macrocyclic complex accompanied by protonation.[20] The similarity of the CO-inhibited nickel active-site structure of [NiFe]/[NiFeSe] hydrogenases to the recently synthesized $[Ni(CO)(SPh)_n(SePh)_{3-n}]^-$ ($n = 0, 1, 2$)[21] complexes has inspired the preparation of derivatives modified in such a way to better mimic the features of the Ni−A/Ni−B, and Ni−SIa/Ni−R states of the catalytic cycle of [NiFe] hydrogenase. Our premise is that information on the structures, stabilities, and reactivity of Ni(II)-exo-thiol and Ni(III)-thiolate complexes could be useful in interpreting the catalytic cycle of H_2 activation in [NiFe] hydrogenase. Herein, we report the synthesis and reactivity of $[Ni(ER)(P(o\text{-}C_6H_4S)_2(o\text{-}C_6H_4SH))]^-$ (ER = SePh (**1**), 2-S−C_4H_3S (**2**)) containing an intramolecular S−H proton directly interacting with both nickel and sulfur atoms by reaction of $[Ni(CO)(ER)_3]^-$ and $P(o\text{-}C_6H_4SH)_3$, respectively. In addition, this report also details our successful efforts toward synthesis of the mononuclear Ni(III) complexes in a sulfur-rich ligation sphere, $[Ni^{III}(ER)(P(o\text{-}C_6H_4S)_3)]^-$ (ER = SePh (**3**), 2-S−C_4H_3S (**4**)), isolated upon exposure of complexes **1** and **2** to O_2, respectively.

Scheme 1

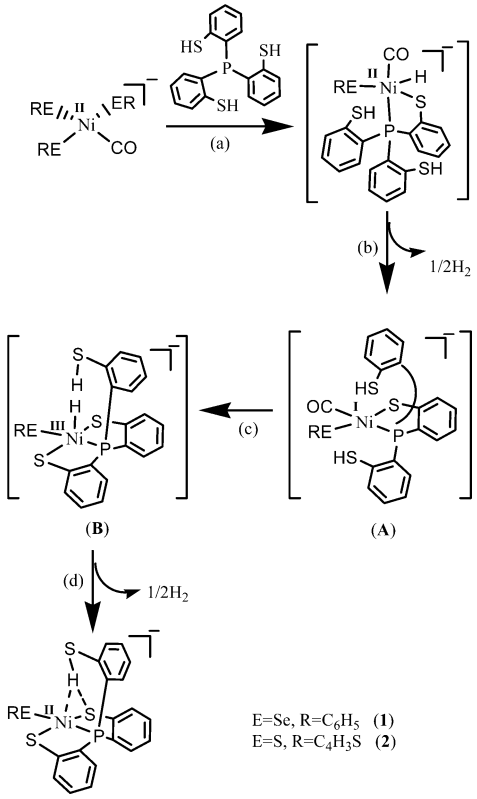

Results and Discussion

Reaction of the $[PPN][Ni(CO)(SePh)_3]$ with tris(2-phenylthiol)phosphine ($P(o\text{-}C_6H_4SH)_3$) in THF at ambient temperature produced the four-coordinate $[PPN][Ni(SePh)(P-(o\text{-}C_6H_4S)_2(o\text{-}C_6H_4SH))]$ (**1**) as a dark red-brown solid isolated in 90% yield.[22] Complex **1** is soluble in THF−CH_3CN (3:1 volume ratio) and displays extremely air-sensitive in solution but is stable to air for minutes in the solid state. Complex **1** exhibits a diagnostic $^{31}P/^1H$ spectra with the $[P(o\text{-}C_6H_4S)_2(o\text{-}C_6H_4SH)]$ phosphine resonance at δ 68.98 (s) ppm (vs H_3PO_4) (CH_2Cl_2) and the benzene protons resonances at δ 6.92−6.99 (m), 7.59−7.62 (m) ppm (CD_2Cl_2) which are consistent with the Ni(II) having a low-spin d^8 electronic configuration in a square planar ligand field. The magnetic measurement of complex **1** is in accord with the diamagnetic forms. The sequences of reaction given in Scheme 1 reasonably account for the observation. The reductive elimination of diphenyl diselenide accompanied by oxidative addition of S−H bond to $[Ni^0]$ unit (Scheme 1a)[21] and reductive elimination of H_2 from the $[Ni^{II}-H]$ intermediate results in the formation of Ni(I)-exo-thiol intermediate **A** (Scheme 1b). This highly reactive Ni(I) species **A** then triggers the cleavage of the second S−H bond affording the reactive

(14) Ogata, H.; Mizoguchi, Y.; Mizuno, N.; Miki, K.; Adachi, S.-I.; Yasuoka, N.; Yagi, T.; Yamauchi, O.; Hirota, S.; Higuchi, Y. *J. Am. Chem. Soc.* **2002**, *124*, 11628−11635.
(15) Foerster, S.; Stein, M.; Brecht, M.; Ogata, H.; Higuchi, Y.; Lubitz, W. *J. Am. Chem. Soc.* **2003**, *125*, 83−93.
(16) (a) Fan, C.; Teixeira, M.; Moura, J.; Moura, I.; Huynh, B. H.; Le Gall, J.; Peck, H. D., Jr.; Hoffman, B. M. *J. Am. Chem. Soc.* **1991**, *113*, 20−24. (b) Whitehead, J. P.; Gurbiel, R. J.; Bagyinka, C.; Hoffman, B. M.; Maroney, M. J. *J. Am. Chem. Soc.* **1993**, *115*, 5629−5635.
(17) (a) Lenz, O.; Friedrich, B. *Proc. Natl. Acad. Sci. U.S.A.* **1998**, *95*, 12474−12479. (b) Kleihues, L.; Lenz, O.; Bernhard, M.; Buhrke, T. Friedrich, B. *J. Bacteriol.* **2000**, *182*, 2716−2724.
(18) (a) Haumann, M.; Porthum, A.; Buhrke, T.; Liebisch, P.; Meyer-Klaucke, W.; Friedrich, B.; Dau, H. *Biochemistry* **2003**, *42*, 11004−11015. (b) Brecht, M.; van Gastel, M.; Buhrke, T.; Friedrich, B.; Lubitz, W. *J. Am. Chem. Soc.* **2003**, *125*, 13075−13083.
(19) Darensbourg, M. Y.; Lyon, E. J.; Smee, J. *J. Coord. Chem. Rev.* **2000**, *206*, 533−561.
(20) Efros, L. L.; Thorp, H. H.; Brudvig, G. W.; Crabtree, R. H. *Inorg. Chem.* **1992**, *31*, 1722−1724.
(21) (a) Liaw, W.-F.; Horng, Y.-C.; Ou, D.-S.; Ching, C.-Y.; Lee, G.-H.; Peng, S.-M. *J. Am. Chem. Soc.* **1997**, *119*, 9299−9300. (b) Liaw, W.-F.; Chen, C.-H.; Lee, C.-M.; Lee, G.-H.; Peng, S.-M. *J. Chem. Soc., Dalton Trans.* **2001**, 138−143.
(22) Block, E.; Ofori-Okai, G.; Zubieta, J. *J. Am. Chem. Soc.* **1989**, *111*, 2327−2329.

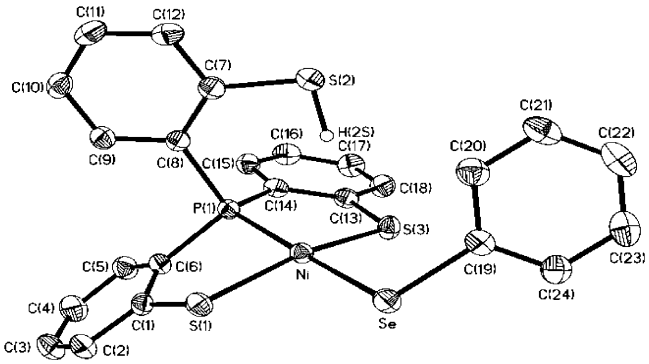

Figure 1. ORTEP drawing and labeling scheme of the [Ni(SePh)(P(*o*-$C_6H_4S)_2$(*o*-C_6H_4SH))]$^-$ anion. Selected bond distances (Å) and angles (deg): Ni−S(3) 2.1648(8); Ni−S(1) 2.2127(8); Ni−Se 2.3349(5); S(3)−Ni−S(1) 162.04(4); P(1)−Ni−Se 174.72(3); S(3)−Ni−Se 93.22(2); S(1)−Ni−Se 92.21(2).

Ni(III)−H intermediate **B** (Scheme 1c).[23] It is presumed that Ni(I) intermediate **A** prefers cleavage of the proposed "agostic $Ni^{I}\cdots H-S$ bond" resulting in the formation of $RS-Ni^{III}-H$ species along with the release of CO as opposed to being stabilized by "η^2-[$Ni^{I}\cdots H-S$] interaction" (Scheme 1c).[24] The subsequent reductive elimination of H_2 from intermediate **B** led to the formation of complex **1** (Scheme 1d).[23] These results establish that the same stoichiometric quantities of $(PhSe)_2$ are formed concurrently with complex **1**.

The infrared KBr solid spectrum of complex **1** shows one broad stretching band (2273 cm^{-1}) in the ν_{S-H} region. The lower energy ν_{S-H} band of complex **1** shifted by ∼215 cm^{-1} from that of the free ligand P(*o*-$C_6H_4SH)_3$ (2488 cm^{-1}) implies the specific [Ni−S···H−S]/[Ni···H−S] interactions. Intramolecular [Ni−S···H−S]/[Ni···H−S] interactions in complex **1** also result in the ^{1}H NMR chemical shift of the SH group, shifting from δ 4.07 (d) ppm ($CDCl_3$) in free ligand P(*o*-$C_6H_4SH)_3$ to δ 8.079 (d) ppm (S−H) (CD_2Cl_2) in complex **1**.[22] The acute C(7)−S(2)−H(2S) bond angle of 97.3(18)° observed in single-crystal X-ray diffraction studies is believed to result from an intramolecular [Ni−S···H−SR] interaction (Figure 1), which supports the observation of the lower IR ν_{S-H} stretching frequency in complex **1**. We noticed that the S(2)···S(3) distance of 3.737 Å in complex **1** is longer than the S(2)···Ni distance of 3.639 Å (Type I, below). Specifically, the S(2)−H(2S) is partially polarized in a sense on the approach of the sulfur atom (S(3)). It is best interpreted in terms of the thiol proton interacting with both sulfur and nickel atoms, where the proton is bound to sulfur and "attracted" between a Ni(II) and the second sulfur atoms, a combination of [Ni−S···H−S]/[Ni···H−S] interactions (Type I, below). In particular, a three-center "agostic" η^2-[Fe−H−S] interaction has been proposed for the protonation of [Fe(SR)-$(CO)_3L]^-$ (L = PEt_3, $P(OEt)_3$),[24] and proton transfer between sulfur and hydride has been observed in $[Ir(H)_2(HS(CH_2)_3SH)$-$(Pcy_3)_2]^+$.[25]

The H/D exchange reaction between complex **1** and D_2O occurred in CH_3CN−THF solution (1:3 volume ratio) at 5 °C

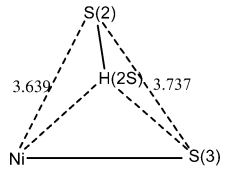

(**I**)

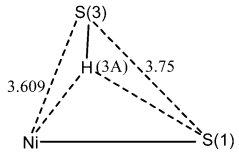

(**II**)

as indicated by IR and ^{2}H NMR. The IR ν_{S-H} at 2273 br cm^{-1} shifting to absorbance at 1676 br cm^{-1} (ν_{S-D}, KBr) is roughly consistent with the calculated position, based only on the difference in masses between S−H and S−D. A ^{2}H NMR resonance that appeared as a broad peak at δ 7.972 (br) (CH_2Cl_2) ppm (using natural abundance of D in CH_2Cl_2 solvent as internal standard, δ 5.32 ppm) was assigned to the S−D resonance, and D_2O was found at 1.601 (br) ppm in the ^{2}H NMR spectrum.

Similarly, the reductive elimination/oxidative addition was also displayed by the reaction of complex [Ni(CO)(2-S−$C_4H_3S)_3]^-$ and P(*o*-$C_6H_4SH)_3$.[21b] When a THF solution of [Ni(CO)(2-S−$C_4H_3S)_3]^-$ was treated with 1 equiv of P(*o*-C_6H_4-$SH)_3$, an immediate change in color of the solution from yellow brown to dark red-brown was observed. The reaction mixture led to the isolation of the extremely air-sensitive red-brown compound [Ni(2-S−C_4H_3S)(P(*o*-$C_6H_4S)_2$(*o*-C_6H_4SH))]$^-$ (**2**) (Scheme 1). In addition to the X-ray analysis, a higher IR ν_{S-H} (2283 cm^{-1} (KBr)) compared to that of complex **1** (2273 cm^{-1} (KBr)) also supports the formation of complex **2**. The ^{1}H NMR spectra of complex **2** show the expected signals for the phenyl and exo-thiol (8.39 (d) (C_4D_8O) ppm) groups involved and display characteristics of diamagnetic d^8 square-planar Ni(II) species. In contrast to complex **1**, the X-ray crystal structure of complex **2** shows that the exo-thiol tends to adopt a [Ni···H−S] interaction (Figure 4). We also noticed that the S(3)···Ni distance of 3.609 Å is much shorter than the S(3)···S(1) distance of 3.75 Å in complex **2** (Type II). It seems unlikely that the thiol proton shuttles between two sulfur atoms or the complete proton transfer results in a six-coordinate d^6 $Ni^{IV}-H$ species in THF solution of complexes **1** and **2** at room temperature. This evidence shows that electronic modulations of the terminally coordinated donor ligand are capable of inducing significantly alternative interaction modes, [Ni−S···H−S], [Ni···H−S], or some mixture thereof. These interactions [Ni−S···H−S], [Ni···H−S], or some mixture may contribute to the stabilization of Ni(II)-exo-thiol complexes **1** and **2**.

Upon addition of dry O_2, a pronounced color change from red-brown to dark green occurs in the CH_3CN−THF solution (1:3 volume ratio) of complexes **1** and **2** at 5 °C, respectively. The UV−vis, EPR, ^{1}H NMR, SQUID, and X-ray diffraction studies confirmed the formation of the mononuclear [Ni^{III}(ER)-(P(*o*-$C_6H_4S)_3$)]$^-$ (ER = SePh (**3**), 2-S−C_4H_3S (**4**)) accompanied by byproduct H_2O identified by ^{1}H NMR (Scheme 2). To unambiguously corroborate the formation of byproduct H_2O, we treated the CH_2Cl_2 solution of [Ni(SePh)(P(*o*-$C_6H_4S)_2$(*o*-C_6H_4SD))] with dry O_2 at ambient temperature. UV−vis spectra are consistent with the formation of complex **3** (also identified by X-ray diffraction) along with the byproduct D_2O found at 1.601 (br) ppm (CH_2Cl_2) in the ^{2}H NMR spectra (using natural abundance of D in CH_2Cl_2 solvent as internal standard, δ 5.32 ppm). The 4.2 K EPR spectra of complexes **3** and **4** are identical and exhibit high rhombicities with three principal *g* values of 2.304, 2.091, and 2.0. There is no ^{31}P hyperfine coupling

(23) (a) Allan, C. B.; Davidson, G.; Choudhury, S. B.; Gu, Z.; Bose, K.; Day, R. O.; Maroney, M. J. *Inorg. Chem.* **1998**, *37*, 4166−4167. (b) James, T. L.; Cai, L.; Mutterties, M. C.; Holm, R. H. *Inorg. Chem.* **1996**, *35*, 4148−4161. (c) Cha, M.; Shoner, S. C.; Kovacs, J. A. *Inorg. Chem.* **1993**, *32*, 1860−1863.
(24) Darensbourg, M. Y.; Liaw, W.-F.; Riordan, C. G. *J. Am. Chem. Soc.* **1989**, *111*, 8051−8052.
(25) Jessop, P. G.; Morris, R. H. *Inorg. Chem.* **1993**, *32*, 2236−2237.

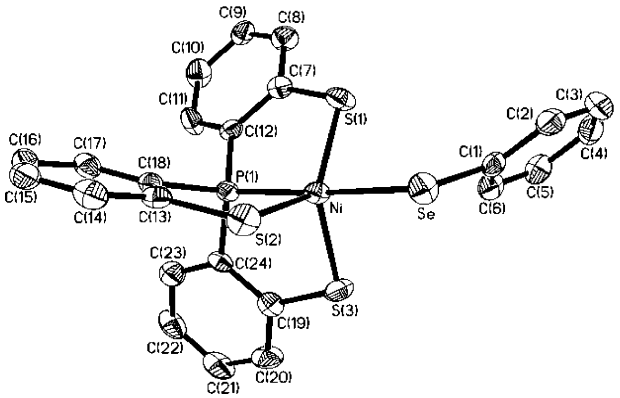

Figure 2. ORTEP drawing and labeling scheme of the $[Ni(SePh)(P(o\text{-}C_6H_4S)_3)]^-$ anion. Selected bond distances (Å) and angles (deg): Ni−P(1) 2.1371(13); Ni−S(1) 2.1944(14); Ni−S(3) 2.2626(14); Ni−S(2) 2.2905(14); Ni−Se 2.3714(8); P(1)−Ni−S(1) 87.41(5); S(1)−Ni−S(3) 129.16(6); S(1)−Ni−S(2) 128.43(6); S(3)−Ni−S(2) 101.88(6); P(1)−Ni−Se 176.60(5); S(1)−Ni−Se 90.51(4).

Scheme 2

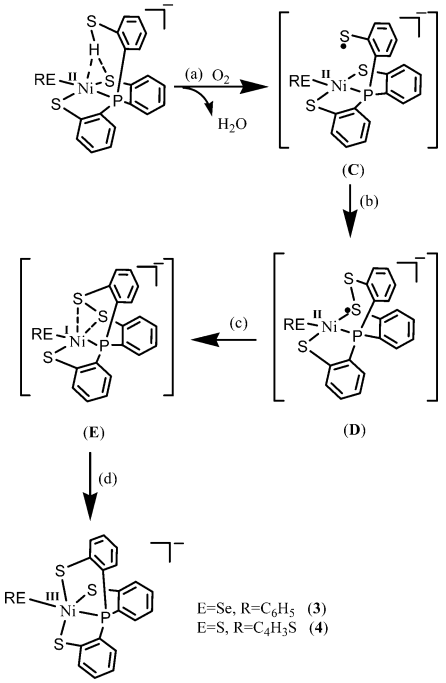

observed under various conditions even in ENDOR detection. Spin quantity of the EPR signal accounts for almost 100% of complex **3**. The average g value ($g_{av} = 2.132$) that is much higher than the spin-only g value 2.0023 indicates large orbital contribution to the paramagnetism, suggesting that the unpaired electron is associated primarily with the nickel ion (Figure 3). These results are consistent with the formation of the Ni(III) oxidation state. The fact that one of the g values is close to the free electron g value suggests a d_{z^2} ground state.[26] The ^{1}H NMR spectra of complexes **3** and **4** at 298 K show the expected paramagnetic properties. The effective magnetic moment in solid state by SQUID magnetometer was 1.85 and 1.91 μ_B for complexes **3** and **4**, respectively, which is consistent with the Ni^{III} having a low-spin d^7 electronic configuration in a distorted trigonal bipyramidal ligand field. The most noteworthy characteristic of complex **3** is the existence of a reversible, metal-

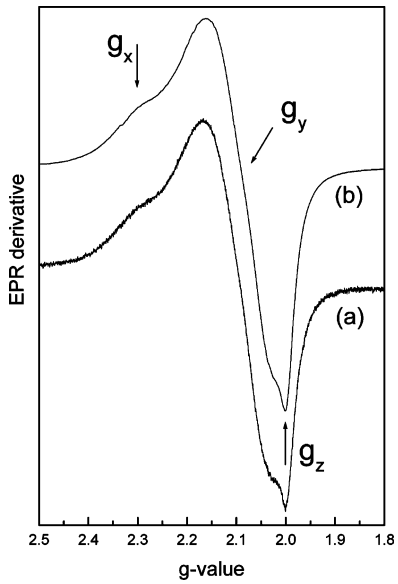

Figure 3. EPR spectra of complexes **3** (a) and **4** (b) frozen in CH_2Cl_2; g values are indicated. Conditions: microwave frequency 9.516 22 GHz, microwave power 2 mW, field modulation 100 kHz, modulation amplitude 4mT, temperature 4.2 K.

based reduction with the $Ni^{III/II}$ redox potential $E_{1/2} = -0.67$ V vs Ag/AgCl ($\Delta E_p = 0.07$ V, scan rate = 0.1 V/s) in MeCN, which is comparable to the $Ni^{III/II}$ redox potentials, ca. −390 to −640 mV vs SCE of [NiFe] hydrogenases.[1] In addition to the X-ray structural analysis, the red-shift absorption bands (595, 954 nm) for complex **4** in the UV−vis spectrum also support the formation of complex **4**.

Results show that complex **2** is much more O_2-sensitive than the corresponding complex **1**.[21] A mechanism proposed to explain the observed formation of complexes **3** and **4** is shown in Scheme 2. Upon contact with dry O_2, the O_2 oxidant has available only the ability of converting the exo-thiol to a thiyl radical (intermediate **C**, Scheme 2) accompanied by byproduct H_2O (Scheme 2a).[27a,b] The rapidly intramolecular addition of a generated thiyl radical to the adjacent sulfur atom of the thiolate ligand yields a Ni(II)-disulfide radical intermediate **D** (Scheme 2b) which rapidly transfers an electron to Ni(II) to produce the Ni(I)-disulfide intermediate **E** (Scheme 2c).[27c] This highly reactive 19-electron Ni(I) species **E** is then driven by the formation of complexes **3** and **4** via an intramolecular oxidative addition of disulfide. Many attempts, based on the EPR monitor of the reaction in THF−CH_3CN (3:1 volume ratio) at low temperature, that were made to detect the intermediates **C**/**D**/**E** were unsuccessful. This proposed mechanism is analogous to the well-known "induced internal electron-transfer reactions"[27a,b] and was successfully employed synthetically by Jaun and coworkers in which cyclization of the photochemically generated thiyl radical yields a sulfuranyl radical accompanied by transfer of a methyl group to Ni(I) to produce a methyl−Ni(II) intermediate.[28]

The stable mononuclear Ni(III)−thiolate **3** and **4** are soluble in CH_2Cl_2 and THF−CH_3CN and form thermally sensitive, air-

(26) Grove, D. M.; van Koten, F.; Zoet, R. *J. Am. Chem. Soc*. **1983**, *105*, 1379−1380.

(27) (a) Stein, C. A.; Taube, H. *Inorg. Chem*. **1979**, *18*, 2212−2216. (b) Branscombe, N. D. J.; Atkins, A. J.; Marin-Becerra, A.; McInnes, E. J. L.; Mabbs, F. E.; McMaster, J.; Schröder, M. *Chem. Commun*. **2003**, 1098−1099. (c) Clark, K. A.; George, A.; Brett, T. J.; Ross, C. R.; Shoemaker, R. K. *Inorg. Chem*. **2000**, *39*, 2252−2253.

(28) Signor, L.; Knuppe, C.; Hug, R.; Schweizer, B.; Pfaltz, A.; Jaun, B. *Chem.−Eur. J*. **2000**, *6*, 3508−3516.

sensitive solutions in organic solvents. On the basis of this investigation and related observations, it is presumed that the polarizable anionic thiolate/selenolate donor ligand and a relatively rigid tetradentate ligand in complexes **3** and **4** place Ni(III) in an optimum electronic condition to minimize the possibility of autoreduction of Ni(III) and prevent formation of polynuclear nickel thiolate species. In the deprotonation study, 10 equiv of triethylamine were required to quantitatively remove the H^+ from anionic complex **1** and transform it into the known Ni(II) dimer $[Ni^{II}(P(o\text{-}C_6H_4S)_3)]_2^{2-}$ (**5**) by removing [SePh]-ligand in THF−CH_3CN at 5 °C.[29]

Figures 1 and 2 display the thermal ellipsoid plot of the anionic complexes **1** and **3**, respectively, and selected bond distances and angles are given in the figure captions. The constraint of the $[P(o\text{-}C_6H_4S)_2(o\text{-}C_6H_4SH)]$ ligand generates 162.04(4)° S(1)−Ni−S(3) angles, enforcing a slight distortion from a square planar at the four-coodinate nickel site ($[NiS_2$-SeP] core) in complex **1**. The geometry and coordination environment around Ni respond rapidly to the oxidation state change of Ni; the geometry of Ni(II) in complex **1** adopts a distorted square planar. In comparison, the geometry of Ni(III) in complex **3** is a distorted trigonal bipyramidal with S(3)−Ni−S(2), S(1)−Ni−S(3), and S(1)−Ni−S(2) bond angles of 101.88(6)°, 129.16(6)°, and 128.43(6)°, individually. The large C(8)−P(1)−Ni angle of 117.14(10)° dramatically differs from the C(6)−P(1)−Ni and C(14)−P(1)−Ni angles of 106.25(11)° and 109.97(11)° found in complex **1**. The significant difference (ΔNi−S = 0.0479(8) Å) of Ni−S bond distances between Ni−S(1) (2.2127(8) Å) and Ni−S(3) (2.1648(8) Å) in complex **1** may be attributed to the "intramolecular [S(2)−H(2S)···S(3)] interaction". The Ni−Se bond length of 2.3349(5) Å in complex **1** is comparable to the Ni(II)−Se bond length of 2.317(2) Å (average) observed in $[Ni(CO)(SePh)_3]^-$.[21] Relative to complex **1**, the mean Ni−Se and Ni−S distances in complex **3** have increased by 0.036 and 0.06 Å, respectively. The strain effect of the chelate ligand in the coordination sphere from complex **1** to **3** (or complex **2** to **4**; from tridentate to tetradentate) overwhelming the contraction effect expected as a consequence of metal-centered oxidation may explain the observed lengthening of the average Ni−S/Ni−Se bond lengths of complex **3**.

ORTEP diagrams of complexes **2** and **4** are shown in Figures 4 and 5, individually. Selected interatomic distances and angles are collected in the figure captions. Bond angles (S(1)−Ni−S(4) 94.43(3)°, S(2)−Ni−S(4) 92.08(3)°, P(1)−Ni−S(1) 89.41(3)°, and P(1)−Ni−S(2) 85.97(3)°) around the Ni(II) of complex **2** define a distorted square planar coordination sphere. The mean Ni−S distance of 2.2001(9) Å in complex **2** falls into the range observed for four-coordinate square planar Ni−thiolate complexes (2.14−2.20 Å)[30] and are within the range of $Ni-S_{cys}$ bond distances observed in the structure of [NiFe] hydrogenase (2.2−2.6 Å).[8b] The geometry around the Ni(III) center of the mononuclear Ni(III) complex **4** is a distorted trigonal bipyramidal. The Ni−S distances (2.215(1), 2.265(1), 2.270(1), and 2.307(1) Å) in this five-coordinate complex **4** are at the upper end of the 2.12−2.28 Å range for oxidized *D. gigas* hydrogenases and have increased by 0.06 Å (average) from complex **2**. The most striking feature of these structures is that complexes **3** and **4** are authentic mononuclear Ni(III) complexes despite the lack of bulky substituents near the sulfur/selenium atoms. The five-coordinate complexes **3** and **4** have the feature of containing four sulfurs (or combinations of three sulfurs and one selenium) and one phosphorus atom. It is these electron-rich functionalities that are primarily responsible for the relative stabilization of the Ni(III) state and the rigidity of the chelating ligand preventing expansion of the coordination sphere to accommodate a sixth, bridging sulfur ligand.

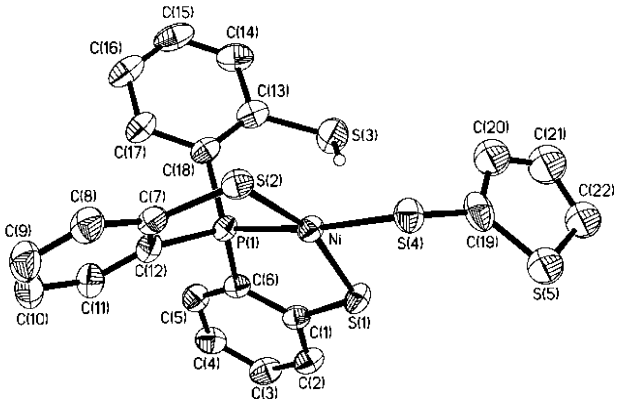

Figure 4. ORTEP drawing and labeling scheme of the $[Ni(2\text{-}S-C_4H_3S)P((o\text{-}C_6H_4S)_2(o\text{-}C_6H_4SH))]^-$ anion. Selected bond distances (Å) and angles (deg): Ni−P(1) 2.1080(8); Ni−S(1) 2.1637(9); Ni−S(2) 2.2137(9); Ni−S(4) 2.2230(9); P(1)−Ni−S(1) 89.41(3); P(1)−Ni−S(2) 85.97(3); S(1)−Ni−S(2) 160.95(4); P(1)−Ni−S(4) 173.32(4); S(1)−Ni−S(4) 94.43(3); S(2)−Ni−S(4) 92.08(3).

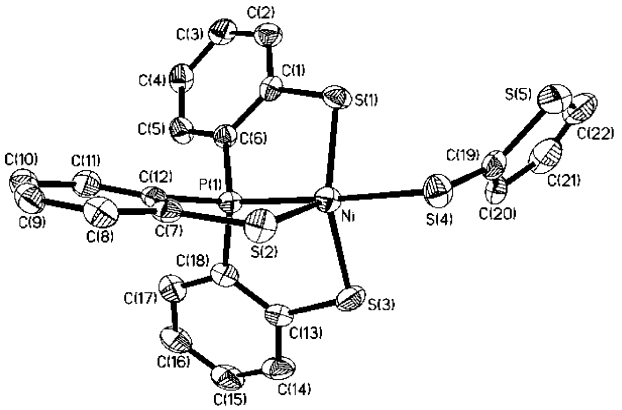

Figure 5. ORTEP drawing and labeling scheme of the $[Ni(2\text{-}S-C_4H_3S)(P(o\text{-}C_6H_4S)_3)]^-$ anion. Selected bond distances (Å) and angles (deg): Ni−P(1) 2.1598(11); Ni−S(1) 2.2147(11); Ni−S(4) 2.2650(12); Ni−S(3) 2.2697(13); Ni−S(2) 2.3069(11); P(1)−Ni−S(1) 86.07(4); P(1)−Ni−S(4) 177.02(5); S(1)−Ni−S(4) 90.98(4); S(1)−Ni−S(3) 133.20(5); S(1)−Ni−S(2) 121.10(5); S(3)−Ni−S(2) 104.76(5).

Conclusion and Comments

Studies on the mononuclear Ni(II)−exo-thiol and Ni(III)−thiolate complexes (**1**−**4**) have led to the following results related to the structure, reactivity, and spectroscopic properties of the nickel site of bimetallic Ni−Fe active site of [NiFe] hydrogenase.

(1) Ni^{II}−exo-thiol complexes **1** and **2** stabilized by an intramolecular S−H proton directly interacting with both nickel and sulfur atoms were synthesized and characterized by IR, ^1H

(29) Franolic, J. D.; Wang, W. Y.; Millar, M. *J. Am. Chem. Soc*. **1992**, *114*, 6587−6588.
(30) (a) Cha, M.; Gatlin, C. L.; Critchlow, S. C.; Kovacs, J. A. *Inorg. Chem*. **1993**, *32*, 5868−5877. (b) Kruger, H.-J.; Holm, R. H. *J. Am. Chem. Soc*. **1990**, *112*, 2955−2963. (c) Mills, D. K.; Reibenspies, J. H.; Darensbourg, M. Y. *Inorg. Chem*. **1990**, *29*, 4364−4366. (d) Baidya, M.; Olmstead, M.; Mascharak, P. K. *Inorg. Chem*. **1991**, *30*, 929−937. (e) Kumar, M.; Colpas, G. J.; Day, R. O.; Maroney, M. *J. Am. Chem. Soc*. **1989**, *111*, 8323−8325. (f) Fox, S.; Wang, Y.; Silver, A.; Millar, M. *J. Am. Chem. Soc*. **1990**, *112*, 3218−3220.

NMR, UV−vis, and X-ray diffraction. The exo-thiol proton in complexes **1** and **2** was identified as a D_2O exchangeable proton from ^2H NMR and IR ν_{S-D} studies and was quantitatively removed by Lewis base Et_3N (10 equiv) to yield the known Ni(II) dimmer, complex **5**.

(2) The distinct electron-donating ability of the terminally coordinated ligands $[SePh]^-$ and $[S-C_4H_3S]^-$ in complexes **1** and **2**, respectively, may serve to regulate the intramolecular [Ni−S···H−S]/[Ni···H−S] interactions or some mixture thereof.

(3) The mononuclear Ni(III) complexes **3** and **4** in a coordination environment containing largely chalcogenolate ligands were obtained upon addition of dry O_2 to **1** and **2** and characterized by EPR, UV−vis, ^1H NMR, SQUID, and X-ray diffraction. Factors contributing to the stability of the distorted trigonal bipyramidal complexes **3** and **4** are attributed to a relatively rigid multidentate ligand and a polarizable anionic chalcogenolate donor ligand sufficient to place Ni(III) in an electron-rich (optimum electronic) condition but insufficient to cause autoreduction of the Ni(III) state and polymerization.

(4) The 4.2 K EPR signals of complexes **3** and **4** with three principal g values of 2.304, 2.091, and 2.0 are compatible with the g values near 2.31, 2.24, and 2.01 (for Ni−A) and 2.33, 2.16, and 2.01 (for Ni−B) ascribed to Ni(III) observed in the oxidized Ni−A as well as Ni−B states of [NiFe] hydrogenases, a formal Ni(III) in a $3(d_{z^2})^1$ electronic configuration.[12b,31] The redox potential $E_{1/2} = -0.67$ V (vs Ag/AgCl) in MeCN is comparable to the $Ni^{III/II}$ redox potentials, ca. −390 to −640 mV (vs SCE) of [NiFe] hydrogenases.[1]

(5) Both complexes **1** and **2** are extremely O_2-sensitive, and replacemeant of selenolate with thiolate ligand in complex **1** has a significant effect on its sensitivity toward O_2. Compared to complex **1**, the less electron-donating thiolate ligand ($[2\text{-}S-C_4H_3S]^-$) coordinated to Ni(II) in complex **2** accelerated the oxidation of complex **2** to yield complex **4** which may implicate that oxidation of complexes **1**/**2** by O_2 occurred, initially, at the exo-thiol instead of the Ni(II) center.

The studies of structures and reactivities of complexes **1**−**4** may lend support to the proposal that the catalytic cycle centered on the nickel site and may be useful for taking into consideration the uptake cycle describing a potential mode of cleaving the H_2 molecule as well as involvement of the cysteine ligand, the hydride formation step, and the cysteine/selenocysteine serving as a role in modulating the catalytic properties of [NiFe]/[NiFeSe] hydrogenases.[5−15] The formation of complexes **1** and **2** possessing a S−H proton directly interacting with both nickel and sulfur atoms via the proposed intermediate **B** $[Ni^{III}(ER)(P(o\text{-}C_6H_4S)_2(o\text{-}C_6H_4SH))(H)]^-$ (ER = SePh, $2\text{-}S-C_4H_3S$) (Scheme 1) implicates that the initial H_2 activation may take place at nickel, and S_{cys} can act either as a proton storage site or as a participant in the promotion of heterolytic H_2 cleavage in [NiFe] hydrogenase.[5−16] Isolation of complexes **1**/**2** suggests that Ni−R/Ni−SIa states may exist as $[(S_{cys}-H)Ni^{II}(S_{cys})_3]$ geometry with a specific $[S_{cys}-H\cdots Ni(S_{cys})_3]$ interaction,[5−16] an interaction thought to stabilize higher valence states of nickel and serve as a proton storage site, and the mononuclear Ni^{III}−thiolate complexes **3**/**4** may reflect the existence of a Ni−A/Ni−B state as a $[(S_{cys})_2Ni^{III}(S_{cys})_2(OH)Fe(CN)_2(CO)]$-coordination environment in [NiFe] hydrogenase. Additionally, this investigation also supports that the [NiFe] hydrogenases are reversibly inactivated upon exposure to O_2,[32,33] as observed in complexes **1** and **2** immediately converting to the Ni(III) state (complexes **3** and **4**) upon exposure to O_2.

Experimental Section

Manipulations, reactions, and transfers were conducted under nitrogen according to Schlenk techniques or in a glovebox (argon gas). Solvents were distilled under nitrogen from appropriate drying agents (diethyl ether from CaH_2; acetonitrile from $CaH_2-P_2O_5$; methylene chloride from CaH_2; hexane and tetrahydrofuran (THF) from sodium benzophenone) and stored in dried, N_2-filled flasks over 4 Å molecular sieves. Nitrogen was purged through these solvents before use. Solvent was transferred to the reaction vessel via stainless cannula under a positive pressure of N_2. The reagents bis(triphenylphosphoranylidene)-ammonium chloride ([PPN][Cl]) (Fluka), iron pentacarbonyl, diphenyl diselenide, cyclopentadienylnickel(I) carbonyl dimer, di(2-thienyl) disulfide, deuterium oxide, 99.9 atom % D (Aldrich), and triethylamine (TCI) were used as received. Compounds tris(2-thiophenyl)phosphine $(P-(o\text{-}C_6H_4SH)_3)$[22] and $[PPN][Ni(CO)(SePh)_3]$/$[PPN][Ni(CO)(2\text{-}S-C_4H_3S)_3]$ were synthesized according to published procedures.[21] Infrared spectra of the ν(CO) and ν(SH) stretching frequencies were recorded on a PerkinElmer model spectrum one B spectrophotometer with sealed solution cells (0.1 mm, KBr windows) or KBr solid. UV−vis spectra were recorded on a GBC Cintra 10e. ^1H and ^2H NMR spectra were obtained on a Varian Unity-500 spectrometer. Electrochemical measurements were performed with CHI model 421 potentionstat (CH Instrument) instrumentation. Cyclic voltammograms were obtained from 2.5 mM analyte concentration in MeCN using 0.1 M $[n\text{-}Bu_4N][PF_6]$ as a supporting electrolyte. Potentials were measured at 298 K vs a Ag/AgCl reference electrode by using a glassy carbon working electrode. Under the conditions employed, the potential (V) of the ferrocinium/ferrocene couple was 0.39 (MeCN). Analyses of carbon, hydrogen, and nitrogen were obtained with a CHN analyzer (Heraeus).

Preparation of Complex [PPN][Ni(SePh)P((*o*-C$_6$H$_4$S)$_2$(*o*-C$_6$H$_4$SH))] (1). A CH_3CN solution (15 mL) of $[PPN][Ni(CO)(SePh)_3]$ (0.547 g, 0.5 mmol) was added to a THF solution (10 mL) of $P(o\text{-}C_6H_4SH)_3$ (0.180 g, 0.5 mmol) by cannula under positive N_2 at 0 °C. The reaction mixture was allowed to warm to room temperature after the reaction solution was stirred for 30 min at 0 °C. The resulting red-brown solution was reduced to 10 mL under vacuum, and diethyl ether (25 mL) was added to precipitate the red-brown solid $[PPN][Ni(SePh)(P(o\text{-}C_6H_4S)_2(o\text{-}C_6H_4SH))]$ (**1**) (0.53 g, 90%). Diffusion of diethyl ether into a THF−MeCN (3:1 volume ratio) solution of complex **1** at −15 °C led to dark red-brown crystals suitable for X-ray crystallography. IR(KBr): 2273 (ν_{SH}) cm^{-1}. ^1H NMR (CD_2Cl_2): δ 8.079 (d) (SH), 6.820−7.344 (m), 7.67 (d) ($P(o\text{-}C_6H_4S)_2(o\text{-}C_6H_4SH)$, SeC_6H_5). ^{31}P NMR (CH_2Cl_2): δ 68.98 ppm (vs H_3PO_4). Absorption spectrum (CH_2Cl_2) [λ_{max}, nm (ϵ, M^{-1} cm^{-1})]: 428 (2960), 510 (1250). Anal. Calcd for $C_{60}H_{48}NP_3S_3SeNi$: C, 64.94; H, 4.36; N, 1.26. Found: C, 64.82; H, 4.44; N, 1.26.

Preparation of Complex [PPN][Ni(2-S−C$_4$H$_3$S)P((*o*-C$_6$H$_4$S)$_2$(*o*-C$_6$H$_4$SH))] (2). Di(2-thienyl) disulfide (0.23 g, 1 mmol) and $[PPN][HFe(CO)_4]$ (0.283 g, 0.4 mmol) were loaded into a 20-mL Schlenk tube and dissolved in THF (5 mL). After being stirred for 15 min at ambient temperature, the solution was transferred to the Schlenk tube containing $[NiCp(CO)]_2$ (0.061 g, 0.2 mmol) by cannula under a positive pressure of N_2. The reaction mixture was stirred for 6 h at ambient temperature, and then hexane (10 mL) was added to precipitate the brown oily product $[PPN][Ni(CO)(2\text{-}S-C_4H_3S)_3]$.[21b] The brown oily product was dried under N_2 purge and redissolved in THF. The yellow-brown solution of $[PPN][Ni(CO)(2\text{-}S-C_4H_3S)_3]$ was then transferred to another Schlenk flask containing $P(o\text{-}C_6H_4SH)_3$ (0.144 g, 0.4 mmol)

(31) Pierik, A. J.; Schmelz, M.; Lenz, O.; Friedrich, B.; Albracht, S. P. *FEBS Lett*. **1998**, *438*, 231−235.
(32) Jones, A. K.; Lamle, S. E.; Pershad, H. R.; Vincent, K. A.; Albracht, S. P. J.; Armstrong, F. A. *J. Am. Chem. Soc*. **2003**, *125*, 8505−8514.
(33) Roberts, L. M.; Lindahl, P. A. *J. Am. Chem. Soc*. **1995**, *117*, 2565−2572.

by cannula under positive N_2 at 0 °C. After the reaction mixture was stirred for 10 min at 0 °C under N_2, degassed hexane (25 mL) was added slowly to precipitate the red-brown solid [PPN][Ni(2-S−C_4H_3S)-(P(*o*-C_6H_4S)$_2$(*o*-C_6H_4SH))] (**2**) (0.201 g, 47%). Diffusion of diethyl ether into a CH_3CN solution of complex **2** at −15 °C for four weeks led to dark red-brown crystals suitable for X-ray crystallography. IR(KBr): 2283 (ν_{SH}) cm^{-1}. ^{1}H NMR (C_4D_8O): δ 8.39 (d) ppm (S−H). Absorption spectrum (CH_2Cl_2) [λ_{max}, nm (ϵ, M^{-1} cm^{-1})]: 440(4320). Anal. Calcd for $C_{58}H_{46}NP_3S_5Ni$: C, 65.17; H, 4.34; N, 1.31. Found: C, 65.04; H, 4.46; N, 1.01.

D/H Exchange for Reaction of Complex 1/2 and D_2O. To a THF−MeCN (3:1, 8 mL) solution of complex **1** (0.11 g, 0.1 mmol) at 5 °C, a 100-fold excess of D_2O (0.18 mL, 10 mmol) was added. The reaction solution containing the mixture solution of complex **1** and D_2O was stirred for 10 min at 5 °C. Diethyl ether (3 mL) was then added slowly to layer above the mixture solution. The flask was tightly sealed and kept in the refrigerator at −15 °C for 1 week. Red-brown crystals [PPN]-[Ni(ER)(P(*o*-C_6H_4S)$_2$(*o*-C_6H_4SD))] (ER = SePh (**1a**), 2-S−C_4H_3S (**2a**)) were isolated (0.09 g, 89% (**1a**)). IR (KBr): 1676 (ν_{SD}) cm^{-1} (**1a**), 1682 (ν_{SD}) cm^{-1} (**2a**). ^{2}H NMR (CH_2Cl_2): δ 7.972 (br) ppm (**1a**) vs $CHDCl_2$ (natural abundance of D in CH_2Cl_2 solvent, δ 5.32 ppm).[34]

Reaction of Et_3N and Complex 1. To a THF−MeCN (3:1 ratio, 8 mL) solution of complex **1** (0.11 g, 0.1 mmol) at 5 °C, a 30-fold excess of Et_3N (0.03 mL, 3 mmol) was added. The mixture solution was stirred for 10 min at 5 °C. Diethyl ether (2 mL) was added slowly to layer above the mixture solution. The flask was tightly sealed and kept in the refrigerator at −15 °C for 1 week. The well-known dark red crystals [PPN]$_2$[Ni$_2$(P(*o*-C_6H_4S)$_3$)$_2$] (**5**) were isolated (0.1 g, 90%) and characterized by single-crystal X-ray diffraction.[29]

Preparation of Complex [PPN][Ni(SePh)(P(*o*-C_6H_4S)$_3$)] (3). Pure oxygen gas (3 mL) was purged through a red-brown THF−MeCN (3:1 volume ratio, 20 mL) solution of complex **1** (0.11 g, 0.1 mmol) at 0 °C. The reaction solution was allowed to warm to 15 °C slowly and stirred for an additional 10 min. The resulting deep-green solution was reduced in volume by N_2 purge, and diethyl ether was then added to precipitate the dark-green solid [PPN][Ni(SePh)(P(*o*-C_6H_4S)$_3$)] (**3**) (0.08 g, 70%). Diffusion of diethyl ether into a THF−MeCN (3:1 volume ratio) solution of complex **3** at −15 °C yielded dark-green crystals suitable for X-ray crystallography. ^{1}H NMR (CD_3CN): δ −3.70 (br), 5.48 (br), 6.73 (br), 7.75 (br), 10.20 (br), 10.27 (br), 12.21 (br) ppm (SePh, *o*-C_6H_4S). Absorption spectrum (CH_3CN) [λ_{max}, nm (ϵ, M^{-1} cm^{-1})]: 594(790), 941(340). Anal. Calcd for $C_{60}H_{48}NP_3S_3SeNi$: C, 64.99; H, 4.27; N, 1.26. Found: C, 64.90; H, 4.25; N, 1.07.

Preparation of Complex [PPN][Ni(2-S−C_4H_3S)(P(*o*-C_6H_4S)$_3$)] (4). Dry oxygen gas (9 mL) was purged through a red-brown THF solution (10 mL) of complex **2** (0.428 g, 0.4 mmol) at 0 °C. The reaction solution was stirred at 0 °C for an additional 15 min, and a significant change in color of the reaction solution from red brown to deep green was observed. Hexane (25 mL) was then added to precipitate the dark-green solid [PPN][Ni(2-S−C_4H_3S)(P(*o*-C_6H_4S)$_3$)] (**4**) (0.30 g, 71%). Diffusion of hexane into a THF solution of complex **4** at −15 °C for 3 weeks led to dark-green crystals suitable for X-ray crystallography. ^{1}H NMR (CD_2Cl_2): δ −3.99 (br), 5.48 (br), 8.42 (br), 9.70 (br), 11.82 (br), 12.62 (br), 13.67 (br) ppm (S−C_4H_3S, *o*-C_6H_4S). Absorption spectrum (CH_2Cl_2) [λ_{max}, nm (ϵ, M^{-1} cm^{-1})]: 384 (10617), 430 (8283), 595 (3100), 790 (911), 954 (1061). Anal. Calcd for $C_{58}H_{45}NP_3S_5Ni$: C, 65.23; H, 4.25; N, 1.31. Found: C, 64.95; H, 4.65; N, 1.02.

EPR Measurements. EPR measurements were performed at X-band using a Bruker EMX spectrometer equipped with a Bruker TE102 cavity and a Bruker VT2000 temperature control unit (120−300 K). For liquid helium temperature measurements, an Oxford ESR910 continuous-flow cryostat (4−200K) was used. The microwave frequency was measured with a Hewlett-Packard 5246L electronic counter. X-band EPR spectra of complexes **3** and **4** frozen in CH_2Cl_2 were obtained with a microwave power of 2 mW, frequency at 9.516 22 GHz, and modulation amplitude of 0.4 mT at 100 kHz.

Magnetic Measurements. The magnetization data were recorded on a SQUID magnetometer (MPMS5 Quantum Design company) with an external 0.5 T magnetic field for complex **3** (1 T for complex **4**) in the temperature range 2 to 300 K. The magnetic susceptibility of the experimental data was corrected for diamagnetism by the tabulated Pascal's constants.

Crystallography. Crystallographic data and structure refinement parameters of complexes **1**, **2**, **3**, and **4** are summarized in the Supporting Information. The crystals of **1**, **2**, **3**, and **4** chosen for X-ray diffraction studies measured 0.27 × 0.23 × 0.06 mm^3, 0.25 × 0.25 × 0.10 mm^3, 0.25 × 0.12 × 0.06 mm^3, and 0.40 × 0.30 × 0.08 mm^3, respectively. Each crystal was mounted on a glass fiber and quickly coated in epoxy resin. Unit-cell parameters were obtained by least-squares refinement. Diffraction measurements for complexes **1**, **2**, **3**, and **4** were carried out on an SMART CCD (Nonius Kappa CCD) diffractometer with graphite-monochromated Mo Kα radiation (λ = 0.7107 Å) and between 1.25° and 27.50° for complex **1**, between 1.25° and 27.50° for complex **2**, between 1.45° and 27.50° for complex **3**, and between 1.46° and 27.50° for complex **4**. Least-squares refinement of the positional and anisotropic thermal parameters of all non-hydrogen atoms and fixed hydrogen atoms (except H(2S) and H(3A) in complex **1** and **2**, respectively) was based on F^2. An SADABS[35] absorption correction was made. The SHELXTL[36] structure refinement program was employed.

Acknowledgment. We gratefully acknowledge financial support from the National Science Council (Taiwan). Authors thank Prof. Hua-Fen Hsu (National Cheng Kung University) for helpful discussions and Miss Hui-Chi Tan for ^{2}H NMR measurements.

Supporting Information Available: Selected bond distances and angles of complexes **1**−**4** (Table S1), crystallographic data of complexes **1**−**4** (Tables S2 and S3), and X-ray crystallographic file in CIF format for the structure determinations of [PPN][Ni(SePh)(P(*o*-C_6H_4S)$_2$(*o*-C_6H_4SH))], [PPN][Ni(2-S−C_4H_3S)(P(*o*-C_6H_4S)$_3$), [PPN][Ni(SePh)(P(*o*-C_6H_4S)$_3$)], and [PPN][Ni(2-S−C_4H_3S)P((*o*-C_6H_4S)$_2$(*o*-C_6H_4SH))]. This material is available free of charge via the Internet at http://pubs.acs.org.

JA048568L

(34) Zhao, X.; Chiang, C.-Y.; Miller, M. L.; Rampersad, M. V.; Darensbourg, M. Y. *J. Am. Chem. Soc.* **2003**, *125*, 518−524.

(35) Sheldrick, G. M. *SADABS, Siemens Area Detector Absorption Correction Program*; University of Göttingen: Germany, 1996.

(36) Sheldrick, G. M. *SHELXTL, Program for Crystal Structure Determination;* Siemens Analytical X-ray Instruments Inc.: Madison, WI, 1994.